Sādhanā (2020) 45:202
https://doi.org/10.1007/s12046-020-01419-w

Multi-objective optimisation of damper placement for improved seismic response in dynamically similar adjacent buildings

M B PATIL[1,*], U RAMAKRISHNA[2] and S C MOHAN[2]

[1]Department of Electrical Engineering, Indian Institute of Technology Bombay, Mumbai, India
[2]Department of Civil Engineering, BITS Pilani, Hyderabad Campus, Hyderabad, India
e-mail: mbpatil@ee.iitb.ac.in

MS received 10 January 2020; revised 13 March 2020; accepted 16 March 2020; published online 8 August 2020

Abstract. Multi-objective optimisation of damper placement in dynamically similar adjacent buildings is considered with identical viscoelastic dampers used for vibration control. An exhaustive search is used to describe the solution space in terms of various quantities of interest such as maximum top floor displacement, maximum floor acceleration, base shear and inter-storey drift. With the help of examples, it is pointed out that the Pareto fronts in these problems contain a very small number of solutions. The effectiveness of two commonly used multi-objective evolutionary algorithms, viz. NSGA-II and MOPSO, is evaluated for a specific example.

Keywords. Multi-objective optimisation; seismic response; dynamically similar adjacent buildings.

1. Introduction

The use of energy dissipation devices to reduce structural vibrations arising due to earthquake excitations has been reported extensively (see [1] for a review). The seismic response of a structure and the cost of implementation depend on the type of dampers, the number of dampers and their locations. A design strategy for connected control technique for two dynamically identical structures with cantilever connection is presented in [2]. Adjacent buildings are described in [3] as a linear discrete system consisting of masses, linear springs and linear passive dampers, and optimal damping configurations are obtained to minimise inter-storey drift using different techniques. In another study [4], particle swarm optimisation (PSO) was used to identify magneto-rheological (MR) dampers to improve the seismic response of the structure. To understand the effect of vibration control, experiments have been conducted on adjacent steel buildings connected with MR dampers, validating the control algorithm [5]. The seismic performance of adjacent buildings and analysis of passive and active control systems were presented in [6], where optimisation was performed using a genetic algorithm. Optimal design mechanism of a hybrid control system for two dynamically similar adjacent buildings (DSABs) exposed to seismic excitation is presented in [7], where a genetic algorithm is used for effective and economic use of passive and active dampers. In [8], PSO is used to obtain the optimal actuator positions for a combined RC structure with a shear wall. In [9], three optimisation methods, viz. differential evolution, Nelder Mead and simulated annealing, were used to find the optimum positions of viscous dampers coupling adjacent buildings with target damping ratio and cost as objective functions. It was found that, with optimal placement, it is possible to use a smaller number of dampers to effectively reduce the seismic response.

From this literature, it is observed that there are limited studies on seismic control of DSABs using the connected control technique. Moreover, in most studies, dynamically similar buildings are differentiated by base isolation or bracing. To the best of the authors' knowledge, optimisation of damper placement for DSABs with respect to multiple objectives has not been presented so far. The purpose of the present study is therefore to explore the effect of damper positions on the seismic response of DSABs using multi-objective (MO) optimisation.

In particular, in this work, we consider two DSABs connected with viscoelastic (VE) dampers. VE dampers are made of VE materials such as rubber polymer layered between steel plates, as illustrated in [10]. VE material exhibits both viscosity and elasticity. VE dampers, when incorporated in the structure, can significantly increase the overall damping of the structure. VE dampers have been successfully incorporated in a number of tall buildings as a viable energy dissipating system to suppress wind- and earthquake-induced motion.

Seismic response of DSABs on a rigid foundation in the presence of VE dampers has been presented in [11–13]. Figure 1 shows the multi-degree freedoms of two six-storeyed DSABs where each floor mass is lumped at a single point. Each dashed line in figure 1c corresponds to two dampers (at either end, as shown in figure 1b). The purpose

*For correspondence

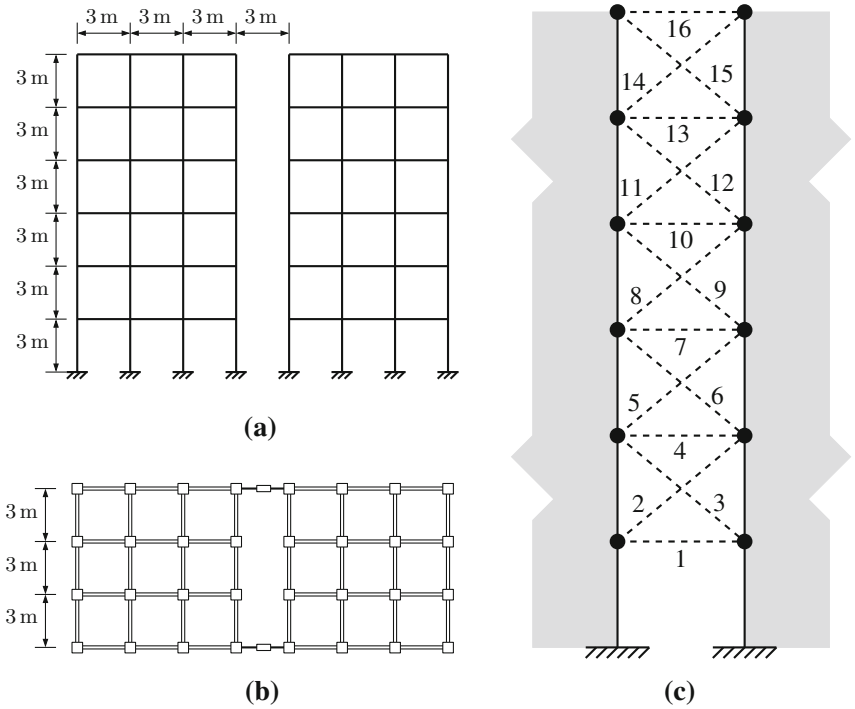

Figure 1. Two DSABs: (**a**) elevation, (**b**) plan and (**c**) schematic representation.

of using dampers is to ensure that certain quantities such as top floor displacement and maximum floor acceleration do not exceed the corresponding limits in the presence of an earthquake excitation. These quantities will depend on the damper parameters, number of dampers and their placement. The focus of this paper is to study the effect of number of dampers and damper placement for a given set of damper parameters.

This paper is organised as follows. We start with a description of the DSAB seismic response problem in section 2. In section 3, we describe the solution space for specific examples. In section 4, we discuss the formulation of the MO optimisation problem and the multi-objective evolutionary algorithms (MOEAs) considered in this work. In section 5, we present results obtained for DSABs with ten storeys and different values of N_d, the number of dampers. In section 6, we compare the performance of three MOEAs in the context of the damper placement optimisation problem. Finally, in section 7, we present conclusions of this work along with some future research directions.

2. Problem description

The equations of motion for two DSABs, without and with dampers, are given by equations (1) and (2), respectively [13], where $\mathbf{C}_D$ and $\mathbf{K}_D$ account for damping and stiffness provided by the VE dampers, respectively:

$$\mathbf{M}\ddot{\mathbf{X}} + \mathbf{C}\dot{\mathbf{X}} + \mathbf{K}\mathbf{X} = -\mathbf{M}\mathbf{I}\ddot{x_g}. \tag{1}$$

$$\mathbf{M}\ddot{\mathbf{X}} + (\mathbf{C} + \mathbf{C}_D)\dot{\mathbf{X}} + (\mathbf{K} + \mathbf{K}_D)\mathbf{X} = -\mathbf{M}\mathbf{I}\ddot{x_g}. \tag{2}$$

A detailed description of equation (2) is given in [13]. The vector $\mathbf{X}$ contains the relative displacement of each floor (in each of the two buildings) due to the ground acceleration excitation given by $\ddot{x_g}$. Several ground accelerations are available in the literature; however, since our emphasis here is on optimisation aspects, we have selected one representative signal, viz., the 1940 El Centro ground acceleration record from strong motion data base [7]. All results presented in this paper are obtained for the El Centro acceleration. It is assumed that the buildings have insignificant plan irregularity with rigid slabs at all floor levels and no off-plane modes.

Equation (2) is solved using Newmark's method [14] to yield $\mathbf{X}(t)$, $\dot{\mathbf{X}}(t)$ and $\ddot{\mathbf{X}}(t)$, i.e., respectively, the displacements, velocities and accelerations of all floors of the left and right buildings. The parameters used in this calculation are as follows. The dimensions are as shown in figure 1. The mass and stiffness are 64,719 kg and 3.7774×10^8 N/m per storey. The VE damper properties are $K_d = 10^6$ N/m and $C_d = 10^8$ N-m/s. Note that the analysis here is carried out by considering linear behaviour of the structure. With the dampers added, the structural parameters (such as

natural frequency and storey shear) are expected to change slightly. As long as these changes are within the allowable limits as per IS 1893, storey drift would not exceed 0.004 times storey height, and the structure would still be safe. Also, for buildings with optimally placed dampers, the storey drifts due to addition of dampers have been calculated, and they have been found to be well within the allowable limits as per standard provisions [15, 16].

Figure 2a shows the top left floor displacement $x_L(t)$ obtained by solving equation (1) for six-storeyed DSABs without dampers. Figure 2b shows $x_L(t)$ for the same DSABs but with two dampers connected as shown in the figure. The reduction obtained in $x_L(t)$ with the use of dampers is clearly seen.

There are several other possible locations for the dampers. The question that naturally arises is whether there is an optimum placement that would lead to smaller displacements (or improved values for any other objective functions). Specifically, in this paper, we consider optimisation of the damper configuration for a given number of floors (N_f) and a given number of dampers (N_d) with the building and damper parameters held constant. To begin with, we take a detailed look at the solution space for a few examples in order to gain some insight regarding the number of optimal solutions.

3. Solution space examples

The solution space for a MO optimisation problem depends on the choice of the objective functions. For the damper placement optimisation problem, various objective functions have been used in the literature [6]. Here, we describe the solution space for three sets of objective functions for six-storeyed DSABs (i.e., $N_f = 6$) with three or four dampers (i.e., $N_d = 3$ or $N_d = 4$).

3.1 *Maximum floor displacements*

In this case, we consider two objective functions, viz. the maximum displacements (over time) of the top left floor and the top right floor, denoted by x_L and x_R, respectively. Figure 3a and b show the solution spaces (i.e., solutions obtained for all possible damper configurations) for $N_d = 3$ and $N_d = 4$. Since the two buildings are dynamically similar, the x_L and x_R values are symmetrically located, as seen in the figure.

A solution p is said to dominate another solution q if all objective function values for p are better than those for q. A solution that is not dominated by any other solution is called a Pareto-optimal solution, and the set of all such solutions is called the Pareto-optimal set or Pareto front.

In figure 3a and b, the Pareto-optimal solutions are marked with squares. Figure 3c and d show the damper configurations corresponding to the Pareto-optimal solutions for $N_d = 3$ and $N_d = 4$, respectively.

A comment on the total number of solutions is in order here. The total number of possible damper positions for $N_f = 6$ is $N_f + 2\,(N_f - 1) = 16$, as shown in figure 1c, and the total number of damper configurations (solutions) with $N_d = 3$ is [3] ${}^{16}C_3 = 560$. The solution space in figure 3a has been obtained by solving Eq. 2 for each of these 560 configurations and recording x_L and x_R in each case. It may be noted that some of the (x_L, x_R) values would overlap, and therefore the number of distinct solutions in figure 3a would be less than ${}^{16}C_3$. Once the entire solution space is found, it is a straightforward matter to compare the solutions with each other to obtain the Pareto front.

When the number of possible configurations becomes much larger, it would take too long to evaluate all of them. Furthermore, as N_f increases, the matrix sizes in Eq. 2 also increase, which implies that the solution time per configuration is also larger. For this reason, the above "enumeration" or "exhaustive search" [3] procedure becomes impractical for many cases of practical interest. In this scenario, MOEAs – which would generally require a much smaller number of function evaluations – provide an attractive alternative.

3.2 *Maximum acceleration and inter-storey drift*

We now consider another set of objective functions, viz. the maximum acceleration $a^{\max}$ and the maximum inter-storey drift [17] $\Delta^{\max}$ (over all floors and time). Figure 4a and b show the solution spaces for $N_d = 3$ and $N_d = 4$, respectively, and figure 4c and d show the damper configurations corresponding to the Pareto-optimal solutions.

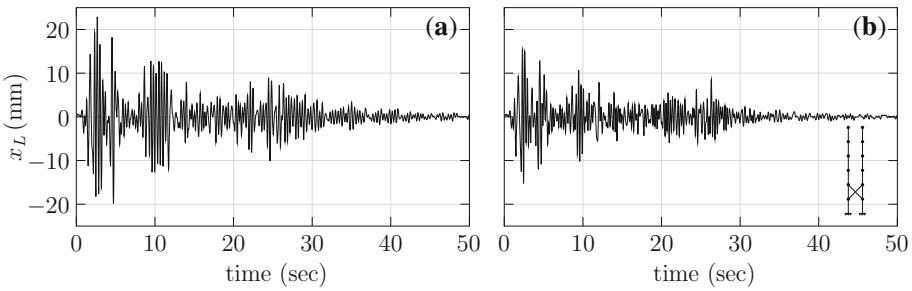

Figure 2. Displacement of top left floor versus time for six-storeyed DSABs as obtained by solving Eq. (2): (**a**) without dampers and (**b**) with dampers connected as shown in the inset.

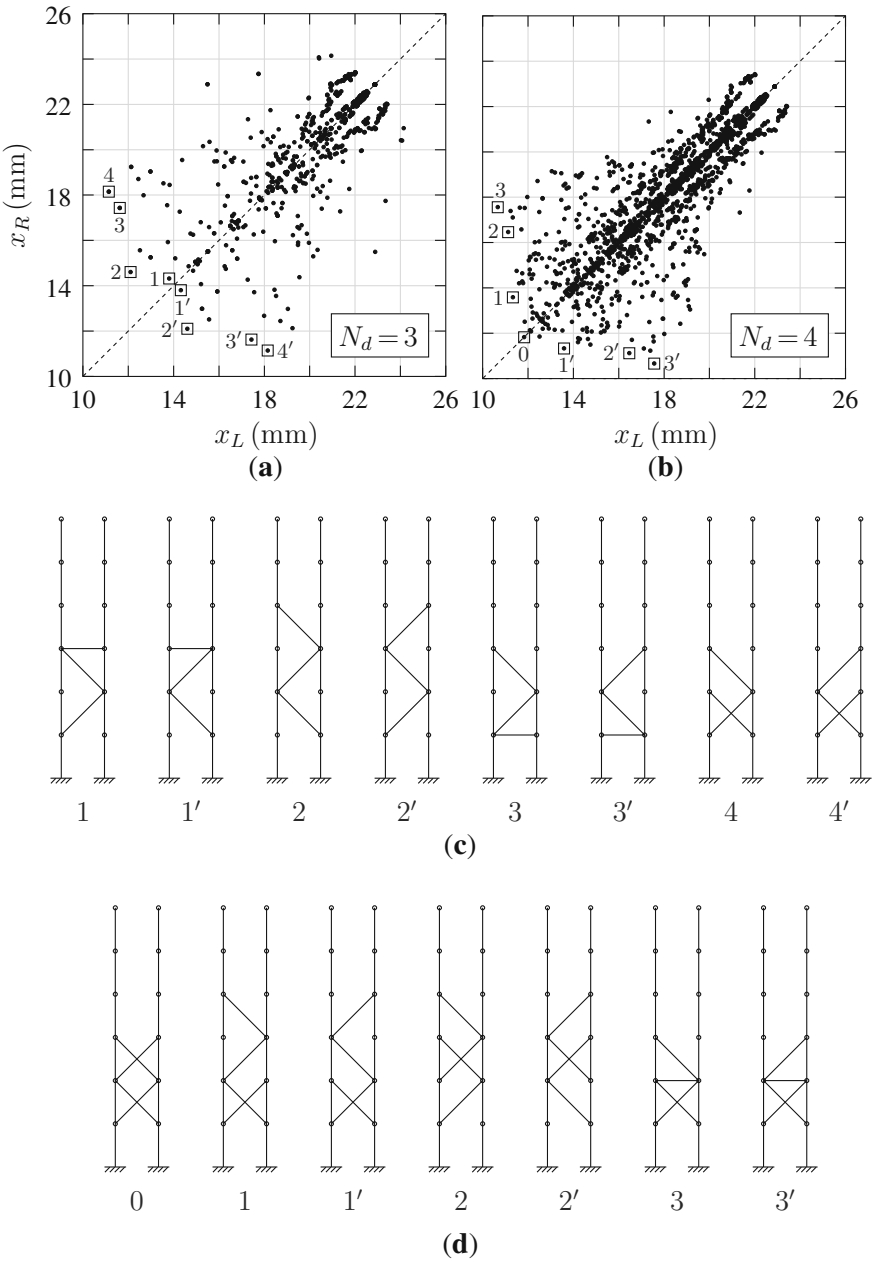

Figure 3. Maximum top left floor and top right floor displacements for six-storeyed DSABs: (**a**) solution space for $N_d = 3$, (**b**) solution space for $N_d = 4$, (**c**) damper placement for Pareto-optimal solutions with $N_d = 3$ and (**d**) damper placement for Pareto-optimal solutions with $N_d = 4$.

3.3 *Maximum top-floor displacement and base shear*

The maximum base shear is yet another quantity of interest [12]. The solution spaces, with the maximum top-floor displacement (over all floors and time) and the maximum base shear (over time) as the two objectives, are shown in figure 5a and b for the same N_f and N_d values as before. The damper configurations corresponding to the Pareto-optimal solutions are shown in figure 5c and d.

From figures 3–5, we observe that the three Pareto fronts have some damper configurations in common. For example, configurations 1 and 1′ of figure 3c also appear in figures 4c and 5c. However, there are other configurations that do not appear in all three Pareto fronts.

The most striking feature of the solution spaces shown in figures 3–5 is the very small number of solutions in the Pareto front. Typically, the performance of an MOEA is evaluated with measures such as generational distance, error ratio and spread [18]. For the

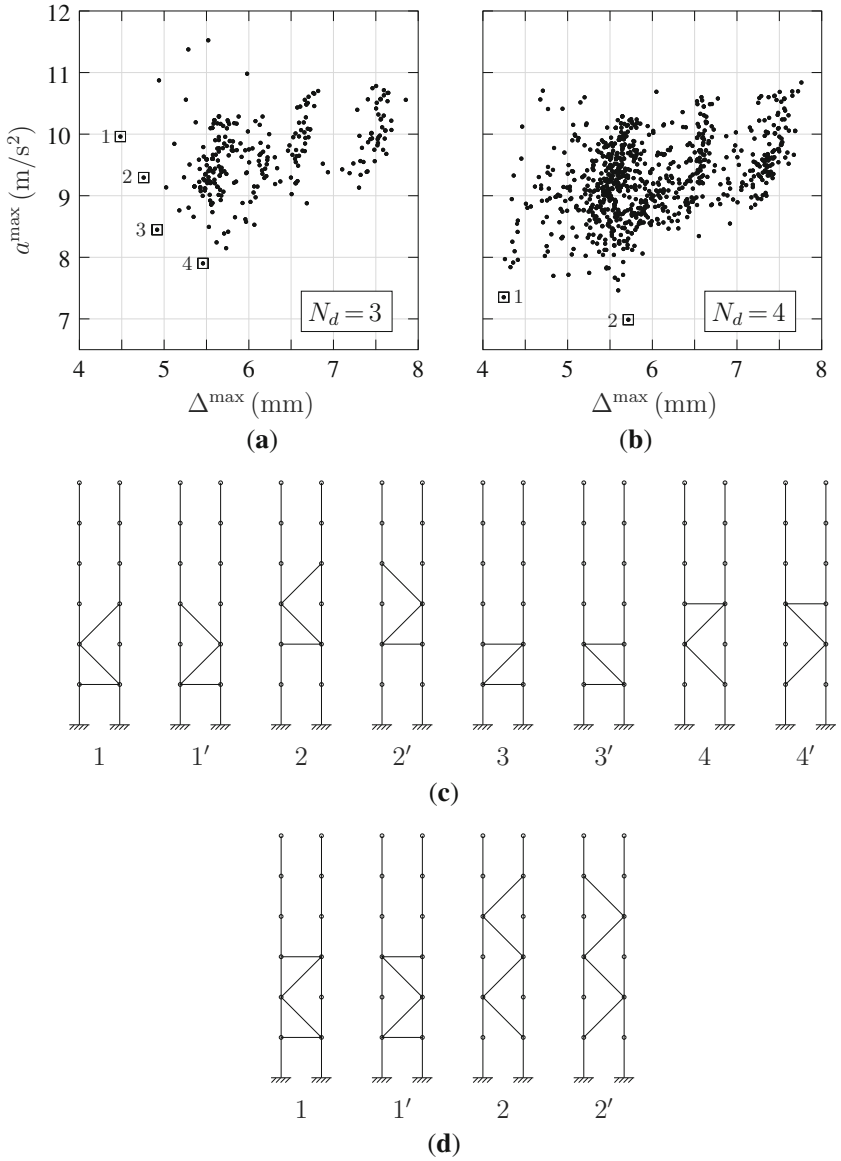

Figure 4. Maximum acceleration and maximum inter-storey drift (over all floors and time) for six-storeyed DSABs: (**a**) solution space for $N_d = 3$, (**b**) solution space for $N_d = 4$, (**c**) damper placement for Pareto-optimal solutions with $N_d = 3$ and (**d**) damper placement for Pareto-optimal solutions with $N_d = 4$.

damper placement optimisation problem considered here, these measures are clearly not applicable. Instead, the most relevant performance measure for this problem is the number of times the MOEA is able to obtain the Pareto-optimal solutions in a given number of independent runs. We will quantify this performance measure in terms of the "success rate" (SR) for the k^{th} Pareto-optimal solution as

$$SR\,(k) = \frac{N_k}{N_r}, \tag{3}$$

where N_r is the number of independent runs (trials) of the MOEA, and N_k is the number of runs in which the k^{th} Pareto-optimal solution was obtained. We will use this definition to compare MOEAs in section 6.

4. Optimisation problem formulation

The MO optimisation problem considered in this paper can be stated as follows. Given two DSABs with N_f floors and N_d identical dampers, find the Pareto-optimal set of

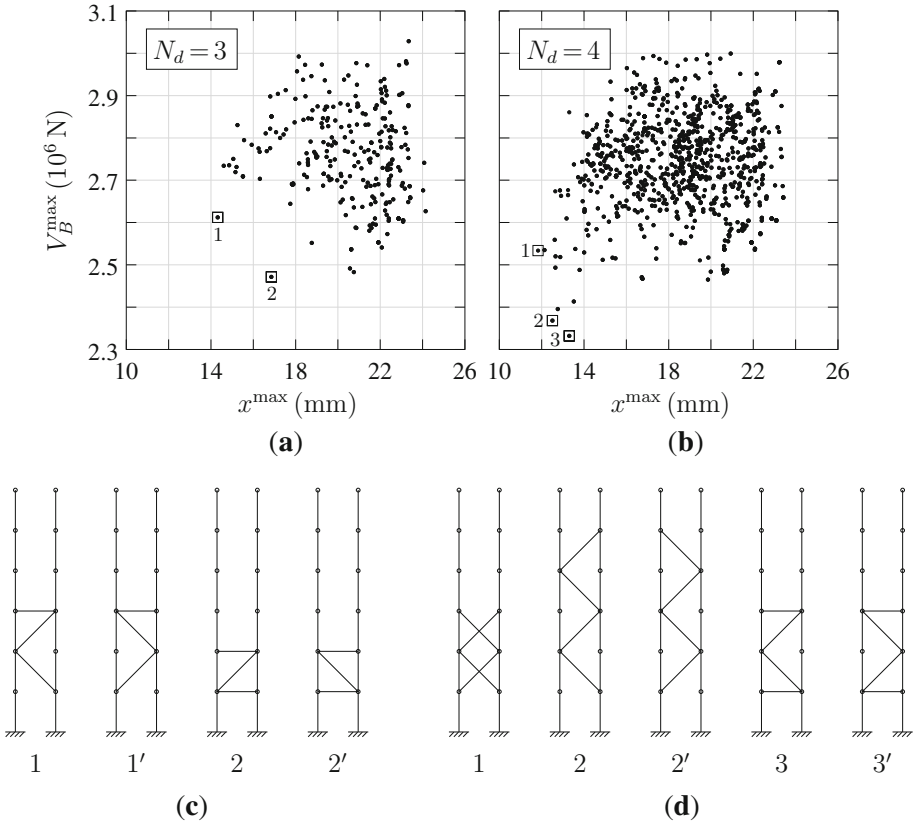

Figure 5. Maximum top-floor displacement (over all floors and time) and maximum base shear (over time) for six-storeyed DSABs: (**a**) solution space for $N_d = 3$, (**b**) solution space for $N_d = 4$, (**c**) damper placement for Pareto-optimal solutions with $N_d = 3$ and (**d**) damper placement for Pareto-optimal solutions with $N_d = 4$.

solutions (damper configurations) with the objectives of minimising f_1 and f_2. We consider two sets of (f_1, f_2):

(i) f_1 is the maximum inter-storey drift ($\Delta^{\max}$), and f_2 is the maximum acceleration ($a^{\max}$), where $\Delta^{\max}$ and $a^{\max}$ are maximum values over time and over all floors. As shown in [19], these two objectives are conflicting in nature, thus making it a MO optimisation problem.

(ii) f_1 is the maximum top-floor displacement ($x^{\max}$), and f_2 is the maximum base shear [12] ($V_B^{\max}$), where $x^{\max}$ and $V_B^{\max}$ are maximum values over time.

Note that several other objective functions have been used in the literature [6]. Here, we have selected two representative sets of objectives. Our main focus is on the optimisation issues involved, and the conclusions drawn from this work are expected to be broadly applicable for other choices of objective functions as well.

We use three MOEAs in this work: NSGA-II [20], MOPSO [21] and MOPSO with a modified mutation scheme. These algorithms are described here.

(a) NSGA-II (see Algorithm 1): This is the real-coded non-dominated sorting genetic algorithm presented in [20]. The following algorithm parameters were chosen: crossover probability $p_c = 0.9$, distribution index for crossover $\eta_c = 15$, mutation probability $p_{\text{mut}} = 1/L$ (where $L = N_d$ is the number of decision variables) and distribution index for mutation $\eta_m = 7$. Since $p_{\text{mut}} = 1/N_d$, on average, one of the damper positions of a given chromosome gets mutated. The following polynomial probability distribution is used for finding the mutated parameter value [20]:

$$P(\delta) = 0.5\,(\eta_m + 1)(1 - |\,\delta\,|)^{\eta_m}. \tag{4}$$

Equation (4) ensures that the new (mutated) parameter value is close to the previous value.

(b) MOPSO-1 (see Algorithm 2): This is the same as the MOPSO algorithm described in [21]. The algorithm parameters used in this work are $W = 0.4$, $C_1 = 2$ and $C_2 = 2$. As described in [21], the mutation operator is implemented as follows. For example, consider a constant probability of mutation $p_{\text{mut}} = 0.05$. In this

case, in each PSO iteration, 5% of the particles (on average) are randomly selected, and for each of them, one of the parameters, i.e. the position of one of the N_d dampers, is randomly mutated.

(c) MOPSO-2: This is identical to MOPSO-1 except for the implementation of the mutation operation. In MOPSO-2, for each particle selected for mutation, one of the parameters is mutated, as in MOPSO-1. However, instead of mutating it randomly, the polynomial probability distribution given by equation (4) is used, with $\eta_m = 7$.

Algorithm 1 NSGA-II

```
Initialize parent population.
Evaluate parent population.
Assign rank and crowding distance to each individual.
for generation = 1 to N_gen do
    Perform selection and crossover.
    Perform mutation.
    Evaluate child population.
    Merge child and parent populations and obtain
      mixed population.
    Perform non-dominated sorting on mixed population
      and obtain the next parent population.
end for
```

Algorithm 2 MOPSO

```
Initialize particle positions, velocities, and
  past best positions.
Initialize external archive.
for ietaration = 1 to N_iter do
    Compute fitness of each particle.
    Update external archive.
    Update past best position of each particle.
    Select global leader from external archive.
    Compute velocity of each particle.
    Move particles.
    Perform mutation.
end for
```

Applying an MOEA to the damper placement problem involves repeated evaluation of the objective functions for specific damper configurations. If the NSGA-II algorithm is used, each chromosome in the population would correspond to a specific damper configuration.

As an example, consider the damper configuration shown in figure 6a. Treating each damper position d_k as a decision variable, the chromosome representing this configuration would be characterised by $d_1 = 2$, $d_2 = 4$, $d_3 = 7$. Similarly, if the MOPSO algorithm is used, the particle representing the configuration in figure 6a would have three parameters, viz. $d_1 = 2$, $d_2 = 4$, $d_3 = 7$.

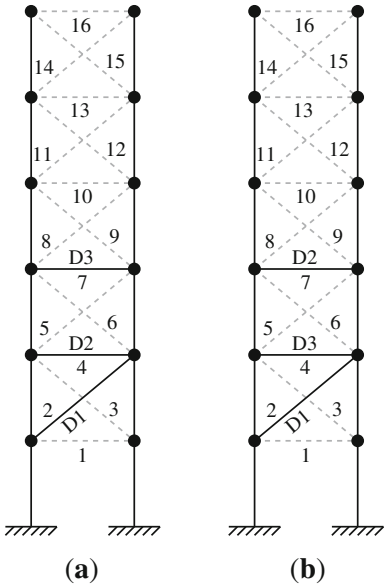

Figure 6. Damper configuration examples for $N_f = 6$, $N_d = 3$.

Since we have assumed the three dampers to have identical properties, the configurations in figure 6a and b would give the same objective function values although their decision variable values differ ($d_1 = 2$, $d_2 = 4$, $d_3 = 7$ in figure 6a, and $d_1 = 2$, $d_2 = 7$, $d_3 = 4$ in figure 6b). Clearly, it is wasteful to evaluate both of these configurations. In order to avoid such repetitive computations, we evaluate a chromosome (or particle) only if the damper positions satisfy $d_3 > d_2 > d_1$. If this condition is not satisfied we assign suitably large values ("penalties") to the objective functions f_1 and f_2, thus making that solution unfit.

Another feature that can be used to limit the search space is the following. For $N_f = 6$ there are a total of 16 possible damper positions, as shown in figure 6a. The first position cannot be occupied by D2 or D3 since D1 needs to occupy a position lower than D2. Similarly, the 16$^{\text{th}}$ position in the figure cannot be occupied by D1 or D2 since D3 needs to occupy a position higher than both D1 and D2. With this logic, we can limit the search space by restricting the decision variables as

$$d_1 \in \{1, 2, \ldots, 13, 14\},$$
$$d_2 \in \{2, 3, \ldots, 14, 15\},$$
$$d_3 \in \{3, 4, \ldots, 15, 16\}.$$

Although the decision variables (d_k) in our problem take on only integer values, we consider them as real variables and convert them to integers before evaluating the objective functions.

5. Optimisation results

We now look at the Pareto-optimal solutions obtained for $N_f = 10$ with different values of N_d. The results presented in this section are obtained with the MOPSO-2 algorithm. We will discuss comparison of the three algorithms presented in the previous section in section 6.

Figure 7 shows the optimal objective function values for the first set of objectives, i.e. $(\Delta^{\max}, a^{\max})$, for $2 \leq N_d \leq 6$, and the corresponding optimal damper configurations. The objective function values for the optimal configurations are also listed in table 1. We observe that, as the number of dampers increases, there is an overall improvement in the objective function values. From table 1, it is also clear that the two objectives, $a^{\max}$ and $\Delta^{\max}$, are conflicting. As a result, the best configuration for minimum $a^{\max}$ is in general different from that for minimum $\Delta^{\max}$, the only exception being the $N_d = 2$ case.

From figure 7 we observe that the optimum configurations take various geometric forms, thus making it difficult to generalise. The complexity would increase further as more objective functions are considered or additional decision variables, such as damper properties, are allowed. For this reason, the use of MOEAs is the only practical option for choosing a damper configuration when the solution space is large. Interestingly, for $N_d = 3$, a large number of optimal configurations ($2A$–$2J$ in figure 7) are found in which the position of the horizontal damper does not change the objective function values.

The Pareto-optimal objective function values for the second set of objective functions, i.e. $(x^{\max}, V_B^{\max})$, are shown in figure 8. The optimal damper configurations are also shown in the figure, and the corresponding objective function values are listed in table 2. For $N_d = 2$, 4, 6, the configuration that results in minimum $x^{\max}$ also gives the minimum $V_B^{\max}$. These "criss-cross" configurations also appear in the Pareto-optimal sets for the first objective set (figure 7) and have been found to be beneficial in the study presented in [13] as well.

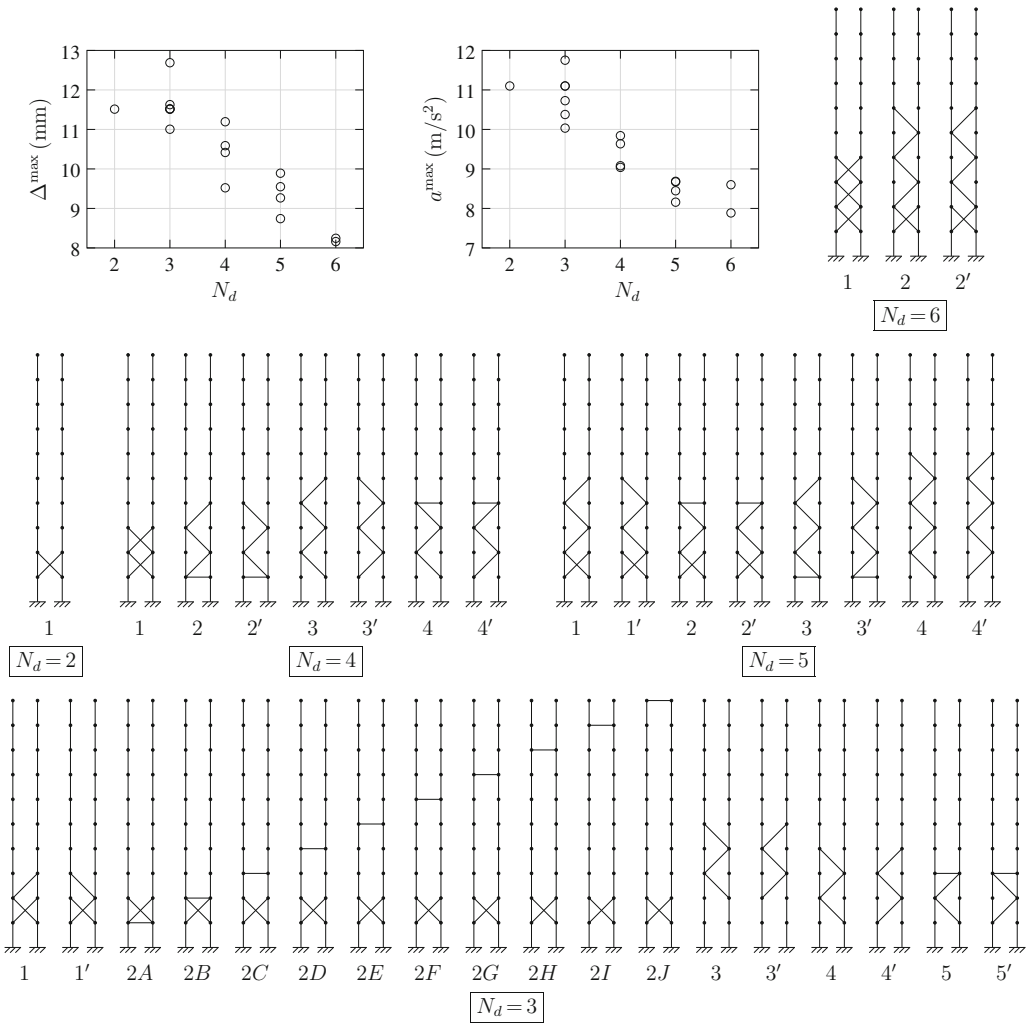

Figure 7. Objective function values for Pareto-optimal solutions of the $(\Delta^{\max}, a^{\max})$ optimisation problem for different values of N_d, and the corresponding optimal damper configurations.

Table 1. Pareto-optimal solutions for the $(\Delta^{\max}, a^{\max})$ optimisation problem, with $N_f = 10$.

N_d	Index	$\Delta_{\max}$ (mm)	$a_{\max}$ (m/s^2)
2	1	11.52	11.10
3	1, 1′	11.01	11.75
	2A-2J	11.51	11.10
	3, 3′	11.52	10.73
	4, 4′	11.63	10.38
	5, 5′	12.69	10.03
4	1	9.52	9.84
	2, 2′	10.42	9.64
	3, 3′	10.59	9.08
	4, 4′	11.20	9.04
5	1, 1′	8.74	8.69
	2-2′	9.27	8.67
	3, 3′	9.55	8.45
	4, 4′	9.89	8.16
6	1	8.16	8.60
	2, 2′	8.25	7.89

Numbers in the index column correspond to the damper configurations shown in figure 7.

Table 2. Pareto-optimal solutions for the $(x^{\max}, V_B^{\max})$ optimisation problem, with $N_f = 10$.

N_d	Index	$x^{\max}$ (mm)	$V_B^{\max}$ (10^6 N)
2	1	64.31	5.21
3	3, 3′	56.76	4.88
4	1	46.92	4.31
5	1, 1′	42.23	4.14
	2, 2′	42.65	4.11
	3, 3′	42.91	4.09
6	1	36.43	3.81

Numbers in the index column correspond to the damper configurations shown in figure 8.

6. Comparison of MOEAs

As the solution space grows, the efficiency of the MOEA becomes very important. Let us take a specific example, viz. $N_f = 10$, $N_d = 6$. In this case the total number of possible damper positions is $N_f + 2\,(N_f - 1) = 28$, and the size of the solution space (the total number of damper configurations) is ${}^{28}C_6 = 376,740$. The average CPU time required for evaluating one configuration was found to be about 6.6 ms using a C program on a Linux desktop computer with 3.8 GHz clock and 8 GB RAM without any parallelisation. Exhaustive search, i.e. evaluation of all possible configurations, would take $376,740 \times 6$ ms or about 41 min. With large values of N_f or N_d the exhaustive search option becomes even more expensive [3], and therefore an MOEA that can obtain the Pareto front solutions by evaluating a small fraction of the solution space is certainly desirable. With this in mind, we define the

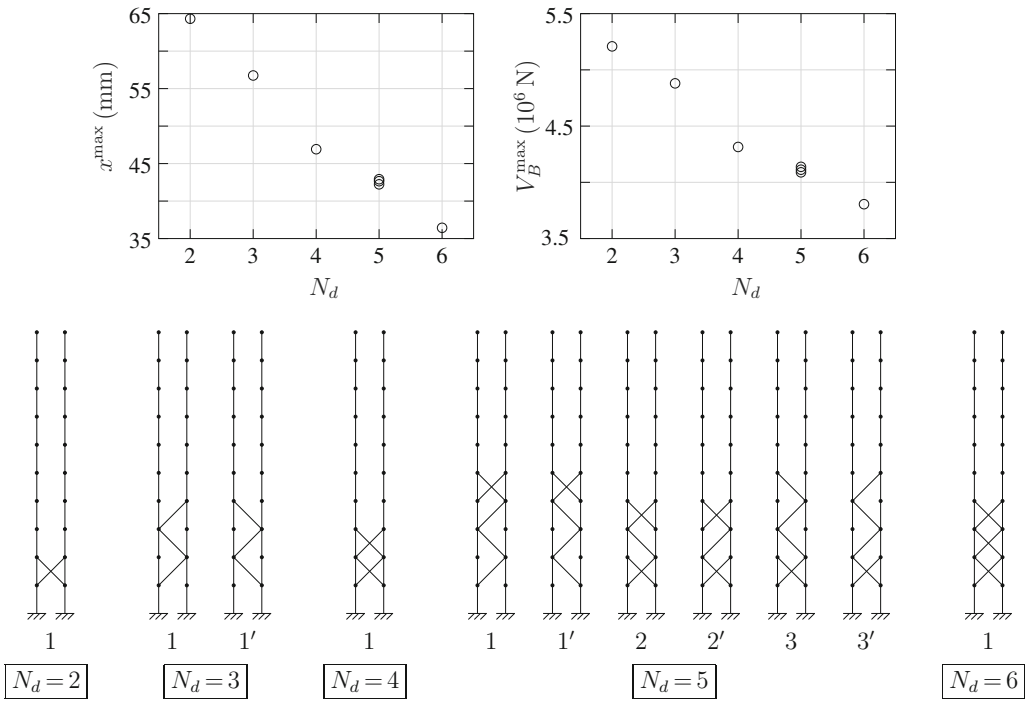

Figure 8. Objective function values for Pareto-optimal solutions of the $(x^{\max}, V_B^{\max})$ optimisation problem for different values of N_d, and the corresponding optimal damper configurations.

following two figures of merit for an MOEA in the context of damper placement optimisation for DSABs.

(a) Computational effort $CE = \frac{N_{FE}^{\text{total}}}{S}$, where N_{FE}^{total} is the total number of function evaluations carried out by the MOEA in N_r independent runs and S is the size of the solution space. Note that exhaustive search, which gives all Pareto-optimal solutions as a by-product, requires $CE = 1$. An MOEA that requires $CE > 1$ for obtaining all Pareto-optimal solutions is therefore of no practical use.

(b) Success rate $SR(k)$, as defined by Eq. 3. An ideal MOEA would find all Pareto-optimal solutions in each run, thus giving $SR(k) = 1$ for each value of k, i.e. for each Pareto-optimal solution. In practice, $SR(k)$ would be smaller.

With these definitions, we can now compare MOEAs to each other. For the same CE, an MOEA with a larger $SR(k)$ is better. Similarly, for the same $SR(k)$, an MOEA with a smaller CE is better.

In the following we will consider the damper placement problem with $N_f = 10$ and $N_d = 6$, and compare the performance of the three MOEAs described in section 4. Several choices exist for the algorithm parameters (such as p_c, η_c, η_m for NSGA-II and W, C_1, C_2 for MOPSO). Here we have selected parameter values given in section 4, which have been found to be effective in the literature.

Apart from the algorithm parameters, the population size N_p (number of chromosomes in NSGA-II or number of particles in MOPSO), the number of iterations N_{iter} and the number of independent runs N_r also play a role in the performance of an MOEA (e.g., see [21]). It is generally not possible to predict which values of N_p, N_{iter}, N_r would be most effective for a given optimisation problem, and some experimentation is required. We have varied N_p, N_{iter}, N_r, and recorded the performance measures in each case. The results are shown in Tables 3 and 4 for the $(\Delta^{\max}, a^{\max})$ and $(x^{\max}, V_B^{\max})$ optimisation problems, respectively. Note that there are three SRs in table 3, corresponding to the three Pareto-optimal solutions shown in figure 7 ($N_d = 6$ case). For example, for the MOPSO-1 algorithm with $N_p = 40$, $N_{\text{iter}} = 200$, $N_r = 30$, $SR(1) = 4/30$, indicating that solution 1 has been found 4 times in 30 independent runs.

We can make the following observations from Tables 3 and 4.

(a) The NSGA-II algorithm consistently misses out one of the solutions (solution 1) in table 3 even with $CE > 1$.

(b) From the first two rows of the NSGA-II section and the first two rows of the MOPSO-1 section of table 3, we find that, by doubling N_{iter}, only SR(2) has improved for NSGA-II whereas both SR(2) and SR(2′) have improved for MOPSO-1.

(c) Compared with NSGA-II, the MOPSO algorithm is generally more effective in obtaining all Pareto-optimal solutions. This observation is similar to that in [22] for a different optimisation problem.

(d) MOPSO-2, which involves the polynomial mutation operator, performs better than MOPSO-1. However, when the mutation probability p_{mut} is increased from 0.05 to 0.2, it fails to capture one of the three solutions in table 3 and the only solution in table 4. The effectiveness of mutation is known to be problem-dependent (e.g., see [21]), and it is generally not possible to predict which mutation scheme and mutation parameters will be the most effective.

Table 3. Summary of performance of NSGA-II, MOPSO-1 and MOPSO-2 algorithms for the $(\Delta^{\max}, a^{\max})$ optimisation problem, with $N_f = 10$ and and $N_d = 6$.

Algorithm	N_p	N_{iter}	N_r	P_{mut}	CE	SR (1)	SR (2)	SR (2′)
NSGA-II	40	200	30	$1/N_d$	0.637	0/30	2/30	4/30
	40	400	30	$1/N_d$	1.274	0/30	2/30	5/30
	100	60	10	$1/N_d$	0.159	0/10	1/10	3/10
	100	120	10	$1/N_d$	0.319	0/10	1/10	4/10
MOPSO-1	40	200	30	0.05	0.637	4/30	4/30	6/30
	40	400	30	0.05	1.274	4/30	5/30	9/30
	40	200	30	0.20	0.637	3/30	9/30	11/30
	40	400	30	0.20	1.274	4/30	9/30	13/30
MOPSO-2	100	60	10	0.05	0.159	2/10	1/10	3/10
	100	60	10	0.20	0.159	0/10	3/10	5/10

Table 4. Summary of performance of NSGA-II, MOPSO-1, and MOPSO-2 algorithms for the $(x^{\max}, V_B^{\max})$ optimisation problem, with $N_f = 10$ and and $N_d = 6$.

Algorithm	N_p	N_{iter}	N_r	P_{mut}	CE	SR (1)
NSGA-II	40	200	30	$1/N_d$	0.637	0/30
	40	400	30	$1/N_d$	1.274	3/30
	100	60	10	$1/N_d$	0.159	0/10
	100	120	10	$1/N_d$	0.319	0/10
MOPSO-1	40	200	30	0.05	0.637	3/30
	40	400	30	0.05	1.274	3/30
	40	200	30	0.20	0.637	4/30
	40	400	30	0.20	1.274	6/30
MOPSO-2	100	60	10	0.05	0.159	3/10
	100	60	10	0.20	0.159	0/10

Figure 9 shows the convergence behaviour of the MOPSO-2 and NSGA-II algorithms for the $(\Delta^{\max}, a^{\max})$ optimisation problem. The plots show the average values (over the population) of the objective functions f_1 and f_2 versus iteration number. The corresponding performance measures are shown in rows 3 and 1, respectively, of the NSGA-II and MOPSO-2 sections in table 3. Note that these two entries in the table are only for 60 iterations whereas the plots in figure 9, for the purpose of illustration, are given

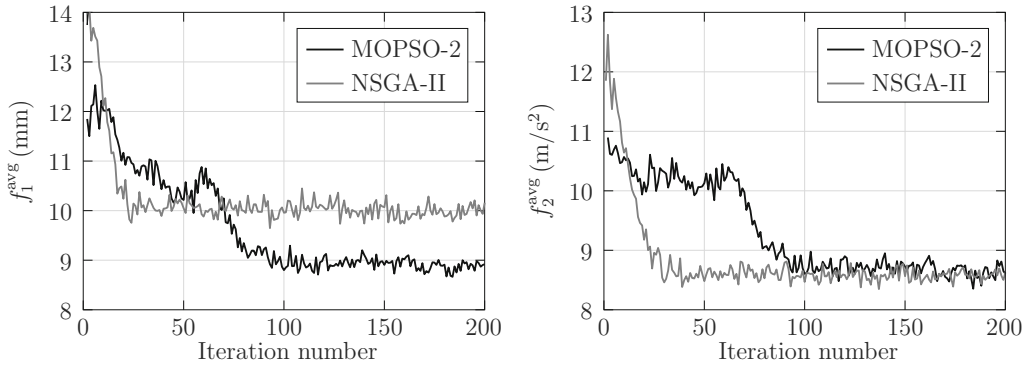

Figure 9. Convergence behaviour of MOPSO-2 (black lines) and NSGA-II (grey lines) for $N_f = 10$, $N_d = 6$ for the $(\Delta^{\max}, a^{\max})$ optimisation problem ($f_1 = \Delta^{\max}, f_2 = a^{\max}$).

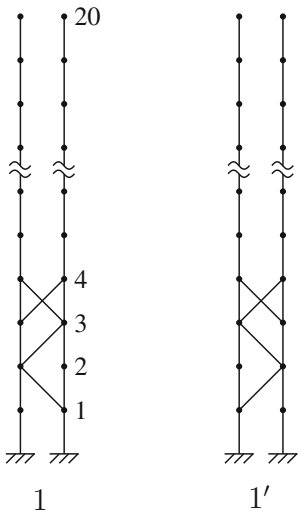

Figure 10. Optimal damper configurations for $N_f = 20$, $N_d = 4$ for the $(\Delta^{\max}, a^{\max})$ optimisation problem.

for 200 iterations. We observe that the NSGA-II algorithm performs better than MOPSO-2 in an average sense since it shows a faster reduction in f_1^{avg} and f_2^{avg} in the initial phase. However, from the entries in the table, we find that the MOPSO-2 algorithm is superior in finding the Pareto-optimal solutions. Judging the algorithm performance from average behaviour would be misleading in this case. This points clearly to the advantage of the performance measures, SR and CE, proposed in this work.

This discussion brings out the need for trying out different MOEAs, possibly with some suitable changes incorporated in the algorithms, for solving a given practical MO optimisation problem. In the literature generally algorithms are evaluated for certain test cases, and results are compared to those of other algorithms. Results of this work suggest that different problems may require different algorithmic options to be explored for improved efficiency.

Finally, we describe an example where the time taken by exhaustive search is much larger than the examples considered so far. Consider the $(\Delta^{\max}, a^{\max})$ optimisation problem with $N_f = 20$ and $N_d = 4$. The total number of possible damper positions for this example is $N_f + 2\,(N_f - 1) = 58$, and the total number of damper configurations with $N_d = 4$ is ${}^{58}C_4 = 424,270$. Exhaustive search takes about 11.5 h whereas MPOSO-2 with $N_p = 100$, $N_{\text{iter}} = 60$, $N_r = 10$ takes only 98 min. The damper configurations obtained by MOPSO-2 in this case are shown in figure 10. By carrying out exhaustive search, we have confirmed that these solutions are indeed the only Pareto-optimal solutions.

7. Conclusions

In this paper, the effect of VE dampers on various quantities of interest related to seismic response of DSABs is considered. The following points are presented for the first time to the best of the authors' knowledge.

(a) A systematic study of the solution space for the DSAB damper placement problem is presented, and it is pointed out that the number of solutions in the Pareto front is very small.
(b) It is argued that, for the DSAB damper placement problem, the figures of merit commonly used for evaluating MOEAs are not meaningful. Two other figures of merit, viz. computational effort and SR, are proposed for comparing the performance of MOEAs.
(c) The effectiveness of MO optimisation in finding optimal damper configurations is clearly demonstrated. Specifically, it is shown that the use of MO optimisation can significantly reduce the computation time as compared with exhaustive search.
(d) The performance of two commonly used MOEAs, viz. NSGA-II and MOPSO, is compared in the context of the DSAB damper placement problem. The MOPSO algorithm with a polynomial mutation operator is shown to be most effective.

The objective of this work was to mainly consider the optimisation aspects of the DSAB damper placement problem. Several related research directions need to be investigated in future, as listed here.

(a) In this work, we have assumed all N_d dampers to have identical parameters (stiffness and damping coefficients). These parameters could also be added to the list of decision variables to give greater flexibility to the decision maker.
(b) We have considered sets of two objective functions. For some problems, it may be desirable to consider three or four objective functions.
(c) A systematic study of the effect of N_d on the best achievable objective values needs to be undertaken. As pointed out earlier [3, 12], a smaller number of dampers with optimal parameters and positions may be adequate to meet the desired specifications. Optimisation can be used to confirm this finding.
(d) Experimental verification of some of the results presented in this paper, especially for small values of N_f and N_d, could be undertaken using a shake table set-up.

Acknowledgements

This work was partially supported by the Science and Engineering Board (SERB), Department of Science and Technology (DST), Government of India. Financial support from DST in the form of Fund for Improvement of S&T Infrastructure (FIST) is also gratefully acknowledged. M.B.P. would like to thank Prof. Kumar Appaiah, IIT Bombay, for discussions related to programming aspects.

References

[1] De Domenico D, Ricciardi G and Takewaki I 2019 Design strategies of viscous dampers for seismic protection of building structures: a review. *Soil Dyn. Earthq. Eng.* 118: 144–165
[2] Makita K, Christenson R E, Seto K and Watanabe T 2007 Optimal design strategy of connected control method for two dynamically similar structures. *J. Eng. Mech.* 133: 1247–1257
[3] Bigdeli K, Hare W and Tesfamariam S 2012 Configuration optimization of dampers for adjacent buildings under seismic excitations. *Eng. Optim.* 44: 1491–1509
[4] Zahrai S M, Akhlaghi M M and Rabipour M 2012 Application of Particle Swarm Optimization for improving seismic response of structures with MR dampers. In: *Proceedings of the International Conference on Noise and Vibration Engineering*, ISMA, pp. 441–448
[5] Basili M, De Angelis M and Fraraccio G 2013 Shaking table experimentation on adjacent structures controlled by passive and semi-active MR dampers. *J. Sound Vib.* 332: 3113–3133
[6] Hadi M N S and Uz M E 2015 Investigating the optimal passive and active vibration controls of adjacent buildings based on performance indices using genetic algorithms. *Eng. Optim.* 47: 265–286
[7] Park K S and Ok S Y 2015 Hybrid control approach for seismic coupling of two similar adjacent structures. *J. Sound Vib.* 349: 1–17
[8] Mastali M, Kheyroddin A, Samali B and Vahdani R 2016 Optimal placement of active braces by using PSO algorithm in near-and far-field earthquakes. *Int. J. Adv. Struct. Eng.* 8: 29–44
[9] Aydin E,Öztürk B and Dikmen M 2017 Optimal damper placement to prevent pounding of adjacent structures considering a target damping ratio and relative displacement. *Omer Halisdemir Univ. J. Eng. Sci.* 6: 581–592
[10] Ramakrishna U and Mohan S C 2020 Performance of low-cost viscoelastic damper for coupling adjacent structures subjected dynamic loads. *Mater. Today Proc.*, https://doi.org/10.1016/j.matpr.2019.12.343
[11] Matsagar V A and Jangid R S 2005 Viscoelastic damper connected to adjacent structures involving seismic isolation. *J. Civ. Eng. Manag.* 11: 309–322
[12] Bhaskararao A V and Jangid R S 2006 Seismic analysis of structures connected with friction dampers. *Eng. Struct.* 28: 690–703
[13] Patel C C and Jangid R S 2010 Seismic response of dynamically similar adjacent structures connected with viscous dampers. *IES J. Part A Civ. Struct. Eng.* 3: 1–13
[14] Rajasekaran S 2009 *Structural Dynamics of Earthquake Engineering*. New Delhi: CRC Press
[15] Ellingwood B 1980 *Development of a probability based load criterion for American National Standard A58: building code requirements for minimum design loads in buildings and other structures*, vol. 13, US Department of Commerce, National Bureau of Standards
[16] Indian Standard 1893 *Criteria for earthquake resistant design of structures*. Bureau of Indian Standards, Part 1
[17] Aydin E 2013 A simple damper optimization algorithm for both target added damping ratio and interstorey drift ratio. *Earthq. Struct.* 5: 83–109
[18] Deb K 2009 *Multi-objective Optimization Using Evolutionary Algorithms*. Chichester: J. Wiley and Sons, Ltd.
[19] Lavan O and Dargush G F 2009 Multi-objective evolutionary seismic design with passive energy dissipation systems. *J. Earthq. Eng.* 13: 758–790
[20] Deb K, Pratap A, Agarwal S and Meyarivan T 2002 A fast and elitist multiobjective genetic algorithm: NSGA-II. *IEEE Trans. Evolut. Comput.* 6: 182–197
[21] Coello C A C, Pulido G T and Lechuga M S 2004 Handling multiple objectives with particle swarm optimization. *IEEE Trans. Evolut. Comput.* 8: 256–279
[22] Barraza M, Bojórquez E, Fernández-González E and Reyes-Salazar A 2017 Multi-objective optimization of structural steel buildings under earthquake loads using NSGA-II and PSO. *KSCE J. Civ. Eng.* 21: 488–500